2013 International Conference on Unmanned Aircraft Systems (ICUAS)
May 28-31, 2013, Grand Hyatt Atlanta, Atlanta, GA

Battery Model-Based Thrust Controller for a Small, Low Cost Multirotor Unmanned Aerial Vehicles

Michal Podhradský, Jarret Bone, Calvin Coopmans
Department of Electrical and Computer Engineering
Department of Mechanical and Aerospace Engineering
Utah State University
Logan, Utah 84321
Email: michal.podhradsky@aggiemail.usu.edu

Austin Jensen
Utah Water Research Laboratory
Utah State University
Logan, Utah 84321
Web: http://aggieair.usu.edu/

***Abstract*—Small Unmanned Aerial Vehicles (UAV) are typically driven by LiPo batteries. The batteries have their own dynamics, which changes during discharge. Classical approaches to altitude control assume time-invariant system and therefore fail. Adaptive controllers require an identified system model which is often unavailable. Battery dynamics can be characterized and used for a battery model-based controller. This controller is useful in situations when no feedback from actuators (such as RPM or thrust) is available. After measuring the battery dynamics for two distinct types of batteries, a controller is designed and experimentally verified, showing a consistent performance during whole discharge test.**

Unmanned Aerial Vehicles (UAV), Vertical Take-Off and Landing (VTOL), quadrotor, hexarotor, multirotor, altitude control, battery monitoring and modelling

I. Introduction

Robust altitude control of a multirotor Unmanned Aerial Vehicle (UAV) is one of the most difficult control problems of Vertical Take-Off and Landing (VTOL) UAVs, most common are quadrotors and hexarotors.

Small low cost UAVs are typically driven by Lithium Polymer (LiPo) batteries, because of their high energy density, high charge and discharge rates, long lifetime, lack of memory effect [1] and affordable cost. Inherent dynamics of Lipo batteries is changing during discharge and affects the flight and control performance. The more the battery is discharged, the less output power it can provide; it slows down actuator response and introduces additional delay to the system.

This change in dynamics affects the UAV's ability to maintain desired altitude. The goal of this paper is to briefly summarize existing methods to overcome this problem and propose a new thrust controller, which takes in account changes in battery dynamics and can set required thrust from actuators without having feedback from them.

First, an overview of UAV platform architecture can be found in Section I-A. A necessary background about UAV control algorithms is given in Section I-B. Introduction to battery modelling is given in Section I-C. A summary of existing solutions is presented in Section II. The proposed controller is described in Section III. The experimental set-up is described in Section IV-A and the laboratory experimental results which prove efficiency are shown in Section V.

A. AggieAir Platform

AggieAir([2],[3]) is a small, low-cost, autonomous, multispectral remote sensing platform [4], which has been developed over the last few years at the Center for Self Organizing and Intelligent Systems (CSOIS) at Utah State University (USU).

AggieAir has reached a stable and robust level in development and has begun work on various

Fig. 1. AggieAir Multirotor Platform – Hexarotor, ready for an indoor flight

Fig. 2. AggieAir Fixedwing Platform – Minion, during landing manoeuvre

applications through a new service center at the Utah Water Research Laboratory (UWRL[5]) at USU. AggieAir utilizes both VTOL and Fixedwing platforms. An example of UAVs, a current hexarotor platform is shown in Figure 1, and a current fixedwing platform is shown in Figure 2. An open-source Paparazzi autopilot[6] is used for flight control, with consumer grade electronics and sensors, while maintaining excellent flight characteristics and reliability [7].

Avionics of such a small low cost UAV consist of Inertial Measurement Unit (IMU), which measures acceleration, angular rate and magnetic field in three axis, Attitude Heading and Reference System (AHRS) which combines IMU measurements and provide attitude estimation, and a GPS sensor providing an absolute position altimeter (altitude above mean sea level), pressure sensors for precise altitude estimation relative to a certain setpoint. Optionally an Inertial Navigation System (INS) which combines measurements from all mentioned

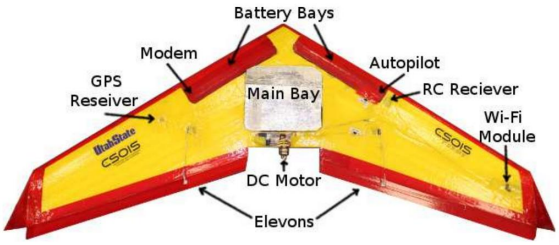

Fig. 3. AggieAir platform overview – Deltawing

sensors are fused together to estimate attitude and position can be used instead of AHRS [8].

In addition a radio transmitter/receiver is necessary for telemetry and remote control. The autopilot unit runs control loops on-board and controls the actuators to keep the desired the attitude and altitude. An overview of the AggieAir system is shown in Figure 3. Control loops of a small VTOL UAV are described in [9].

B. Altitude Control Obstacles

A precise (i.e. within 1 m) altitude control of multirotor UAVs is a complicated problem for two main reasons. First, the altitude estimation is based on noisy measurements. GPS provides absolute position, but its accuracy is rarely better than ± 1 m in perfect conditions. Pressure sensors have resolution of ± 10 cm, but they drift in time and do not provide absolute position. Additional sensors (such as ultrasonic altimeters) can be used, however their use is limited to close proximity of the ground. Second, in altitudes above 20 meters, the UAV is usually subject to strong wind gusts (≥ 10 m/s) and pressure changes[4].

The first problem can be overcome by fusing together GPS, pressure and acceleration measurements. The second problem can be solved by properly tuning the altitude controller.

However, the battery dynamics change in time. It is time-varying system and the controller must account for this transition. If a PID altitude controller is tuned for a fully charged battery pack, it performance will deteriorate during discharge. An outdoor autonomous flight of a hexarotor with constant altitude setpoint is shown in Figure 4. The precision is ± 1 m (with a few outliers caused

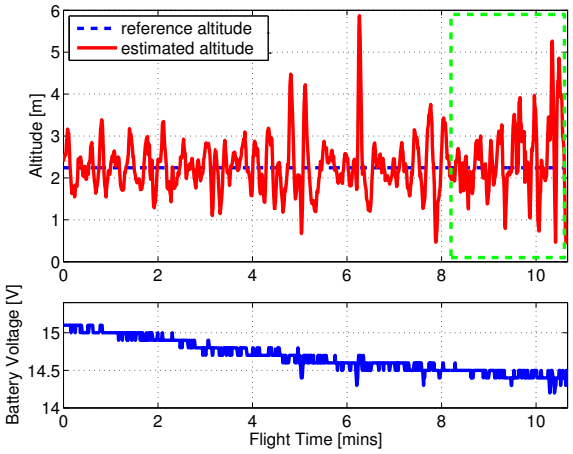

Fig. 4. TOP: Altitude Tracking During Autonomous Outdoor Hexarotor Flight – the green box shows increasing oscillations. BOTTOM: Closed Loop Battery Voltage

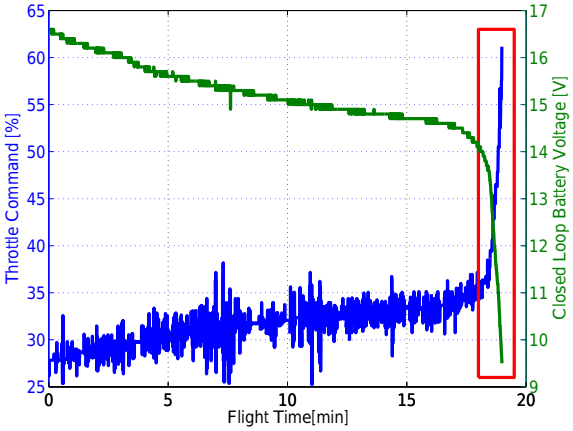

Fig. 5. Change in Throttle Command During Indoor Hexarotor Flight – the red box shows where the battery is starting to collapse

by large wind gust) until around 8th minute, when the performance degrades and the flight has to be terminated.

The significance of the battery dynamics can be seen in Figure 5. It shows a radio controlled indoor flight of a hexarotor at constant altitude. A 4-cell LiPo battery is fully charged at the beginning, and discharges during this 19 minute flight. The pilot has to continuously increase throttle command to keep constant power output from the battery and thus constant altitude. During the flight, the pilot had to increase the throttle by around 10% (comparing the beginning and end of flight). After 18th minute of flight, the battery voltage suddenly drops as the battery is almost completely depleted and the voltage begins to collapse. Before the hexarotor had landed the voltage dropped even below the minimal recommended limit for LiPo batteries, 12V (3V for each cell) which could damage the battery.

Clearly it is important to know the battery state of charge for safety reasons, as well as adjust the control according to the battery dynamics.

C. Battery Model

The key variable describing a battery is State Of Charge (SOC). SoC is the percentage of the maximum possible charge that is present inside a rechargeable battery[10].

Extensive work in battery state estimation has been done for Hybrid Electric Vehicles (HEV, see [1][11][12] for more details) and outcomes of that research can be used as a fundamental base for small low cost UAV applications. In this work the detailed battery models will be omitted because of their complexity and dependency on proper model parameter selection. Instead a relation between actuator output thrust and battery SOC will be established. This approach gives the same benefits as fully identified battery model, however is much simpler and more straightforward.

Maximal battery capacity decreases in time, so does battery power output[13]. For purpose of this work, only new batteries are assumed.

II. Comparison of Existing Solutions

In this Section the most common multirotor altitude control methods are compared. They can be divided into Classical Control (PID regulator with feedforwad) which assumes Linear Time Invariant (LTI) system and Adaptive Control which tackles the problem of time-varying system.

There is a number of vision-based ([14][15]) and visual servoing altitude control techniques ([16][17]) which can be implemented. However, they are not investigated in this work, because the typical mission is assumed to be outdoors, in higher altitudes (up to hundreds of meters) and in rural area or wilderness. In such environments it is hard to guarantee sufficient amount of distinct fea-

tures in the camera image during whole mission, which would affect the control performance.

A. Classical Control

The most common altitude control system used in multirotor UAVs is a PID regulator with feedforward terms. Feedforward is set manually and gives a baseline of thrust to be applied to keep a UAV in constant altitude because the PID feedback control input is small in comparison with nominal thrust. Although very simple, this technique does not provide acceptable performance because the real system is time-variant. In other words, if the controller is tuned for full battery pack, performance degrades with depleted battery, as can be seen in Figure 4.

The main advantage of classical control is simplicity (no system model required, can be tuned experimentally). However it can be used only for application with weak requirements on altitude control.

B. Adaptive Control

Unlike simple PID control, adaptive controllers require a kind of system model. Although a model of multirotor dynamics is known([9][18]), identifying the model is a tedious process. The actuator, consisting of an Electronic Speed Controller (ESC) and a brushless DC motor, can be identified separately from the rest of the system [19] if necessary.

Adaptive control approaches can be divided as follows:

1) PID + Adaptive Feedforward: The aforementioned PID controller can be augmented with adaptive feedforward. Adaptively estimated is nominal thrust, required for hover. Full model and more details are given in [6]. A Kalman filter with kinematic model is used, so no knowledge about the multirotor model is necessary. However, the controller still has to be tuned for a specific airframe.

2) Model Predictive Control: Model Predictive Control (MPC) is another option for altitude control. Although promising better performance, it requires full model of the UAV, which can be difficult to obtain [20].

3) Sliding Mode Control: Another popular control solution is sliding mode control ([21][22]). Again, an identified model of the UAV is required.

III. Battery Model-Based Controller

A battery-based controller extends the PID controller with constant feedforward (see Section II-A) with a term compensating for battery dynamics. The advantage is that no model of the system is needed, only the actuator and battery have to be characterized.

Actuators can be represented by a first-order plus delay transfer function [19]. In this paper, the transfer function is assumed to be unity. ESCs in the actuator take the Pulse Width Modulation (PWM) command from controller and translate it into switching frequency of Field-Effect Transistors (FETs). The higher the switching frequency, the more current is drawn from the battery and the motor spins at higher Revolutions Per Minute (RPM). However, if the current source is not ideal (e.g. a battery), the available current might be limited.If the battery cannot supply enough power, the RPM of motor will decrease and so does thrust produced by the propeller. Most ESCs on the market are open-loop and cannot compensate such a change. In that case the battery dynamics must be characterized.

The proposed controller has a single gain term depending on SOC. Mathematically it can be expressed as (assuming a PID controller with

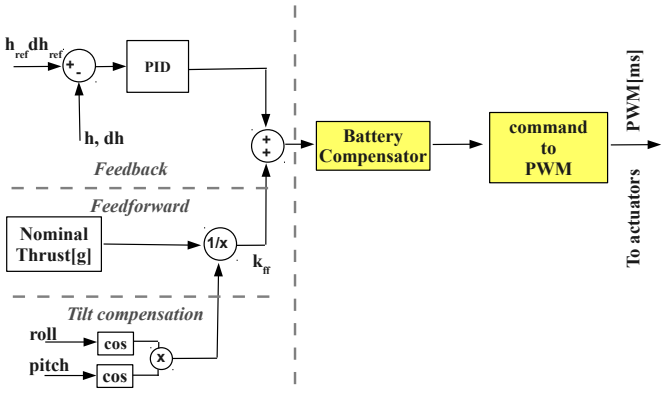

Fig. 6. Battery Based Altitude Control Diagram – with the battery compensation block

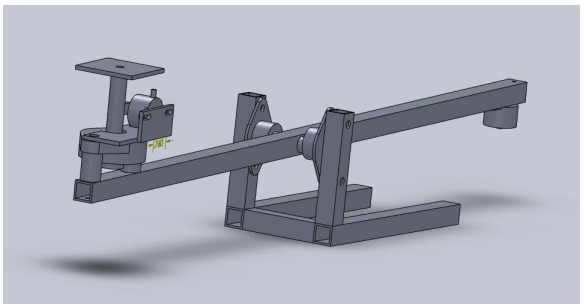

Fig. 7. 3D Model of the Test Bench

feedforward):

$$u(t) = \left(k_p e + k_I \int_0^t e(\tau) d\tau + k_D \frac{de(t)}{dt} + k_{ff} \right) k_b(SOC)$$

Figure 6 shows block diagram of the proposed controller. The feedback section and tilt compensation is unchanged, and the battery compensation block (function $k_b(SOC)$) is added to the feedfoward line. The battery dynamics measurements are described in next section. The main advantage is that the controller compensates for changes in time-varying system and its performance is consistent. The actual function $k_b(SOC)$ is to be characterized in the next section.

IV. Battery Modelling

In order to design a battery-based controller, the battery dynamics must be measured. For this reason an experimental testbench was built and batteries were characterized.

A. Instrumentation

In order to measure thrust of the actuators and SOC of the battery, a testbench based on [19] was developed. The data acquisition and interface to sensors is done by an Arduino MEGA 2560 with a custom expansion board. The tesbed solid model is shown in Figure 7.

Force (Measurement Specialities FC2231) and current (Allegro MicroSystems ACS756SCA-050B) analog sensors are filtered with Resistor-Capacitor filters to prevent excessive noise. The force sensor error is $\pm 3.25\%$, the current sensor error is $\pm 5\%$ according to datasheets. The whole system captures data at 12 Hz and sends them to the computer via USB, with post-processing done

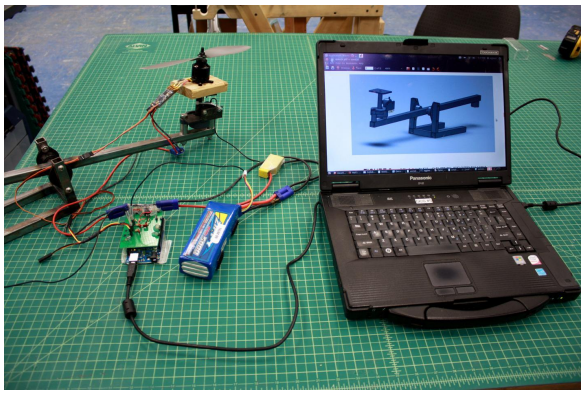

Fig. 8. Experimental Setup: Testbench, Arduino Board and Computer

Fig. 9. Top: Zippy 5000mAh 40C 4-cell, Bottom: MaxAmps 11000mAh 40C 4-cell Lipo batteries

in MATLAB. The actuator consists of Mystery 40A ESC, T-motor MT2814 KV770 motor and 12×3.8" propeller, which is a suitable combination for quad or hexarotor. The ESC is controlled from an Arduino PWM port at 50 Hz rate. The complete testbed prepared for the measurement is shown in Figure 8.

Two different 4-cell LiPo batteries were used: Zippy 5000mAh 40C and MaxAmps 11000mAh 40C. Both batteries are shown in Figure 9.

B. Experimental Set-Up

In order to measure battery dynamics, the following experiment was conducted. The actuator was set to a constant throttle of 55% ($PWM = 1.54$ ms), which produces around 1000 grams of thrust for a fully charged battery. The change in

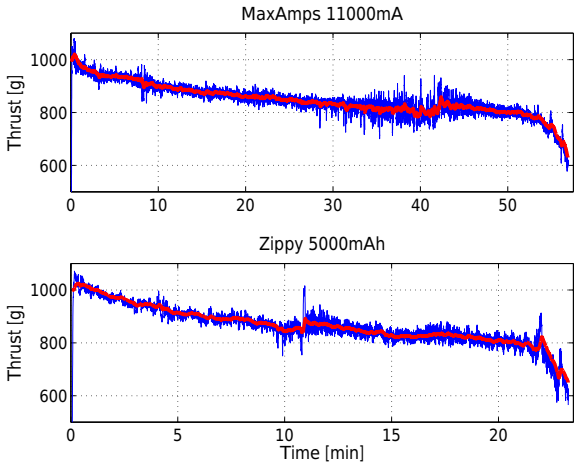

Fig. 10. Battery Discharge Experiment – thrust variations during discharge (BLUE: raw data, RED: filtered data). Filtered with Exponential Moving Average (EMA) filter, $\alpha = 0.01$

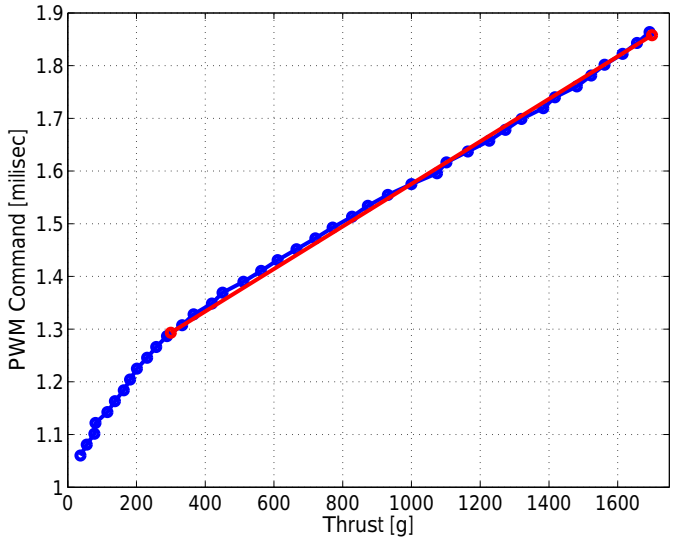

Fig. 11. Dependency of thrust on PWM command width (Mystery 40A ESC, T-motor MT2814 KV770 motor and 12×3.8 propeller), BLUE: measured data, RED: linear approximation

throttle was measured as well as current and battery voltage. The experiment ran until the battery was depleted, which was clearly marked by a sudden decrease in battery voltage, right before the collapse (i.e. until the closed loop voltage dropped below 12 V).

Measured battery discharge current was integrated as:

$$Q_i(t) = \int_0^t i_b(\tau) d\tau \tag{1}$$

The percentage of remaining SOC is defined as [23]:

$$SOC(t) = 100 \left(\frac{Q_c - Q_i(t)}{Q_c} \right) \tag{2}$$

where Q_c is the maximal current capacity present when $SOC = 100\%$.

Note that as the batteries were new, their nominal maximal capacity was used. The discharge experiment is shown in Figure 10. The thrust is proportional to the battery power output $F(grams) \propto P(Watts) = I(Ampers) \times U(Volts)$.

To obtain conversion from grams of thrust to PWM command, the actuator must be characterized [19]. Such conversion is necessary for the experimental verification of the controller, when thrust setpoint (instead altitude) is used (see Section V). The actuator was connected to a power supply, simulating a fully charged battery. PWM command was changed to cover whole admissible range of the ESC (1.1–1.9ms) and produced thrust was measured. The data for each command step were averaged to obtain the resulting plot in Figure 11. The measured data were approximated with a linear function ($y = ax + k$, $a = 4.0323 \times 10^{-4}, k = 1.1722, x \in (300, 1700)$) to avoid nonlinearity.

C. Battery Modelling

The noisy force an current measurements were interpolated using least-squares approximation to obtain dependency of thrust on SOC. The end of the battery pack is considered when the closed-loop-voltage (CLV) drops below 12 V. Knowing the 5% measurement error of the current sensor, the estimated SOC aligns well with the battery capacity. Due to the inherent error in measurements, the flight should be terminated at 10% SOC, so the observed voltage drop does not occur.

The dependency of produced thrust on battery SOC is shown in Figure 12. The overall change in thrust (100%-10% SOC) is about 20% for MaxAmps battery and about 25% for Zippy battery. The thrust curve is almost linear on this range of SOC, except for an exponential drop from fully charged battery to 90%, and then another drop before the battery collapses (below

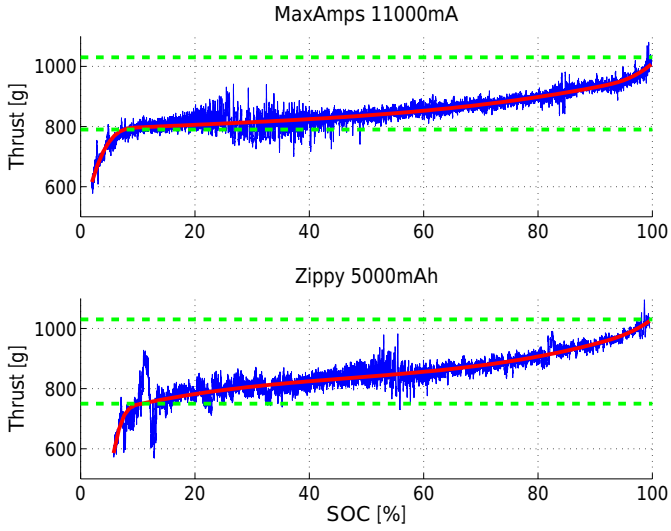

Fig. 12. Thrust dependency on SOC (BLUE: raw data, RED: least-square spline approximation, GREEN: Thrust at 10% and 90% SOC)

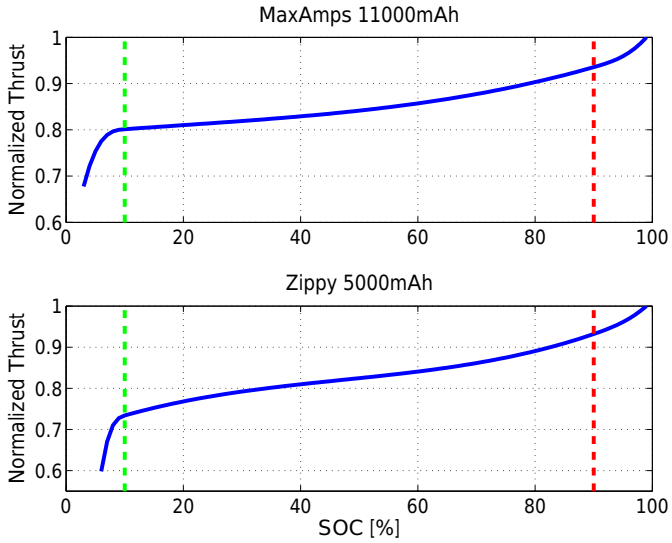

Fig. 13. Normalized spline approximation of the dependency of thrust on PWM command (GREEN: 10% mark, RED: 90% mark)

TABLE I. LEAST-SQUARES SPLINE APPROXIMATION FOR THRUST MEASUREMENTS

Order	# Knots	Knot 1	Knot 2
4	2	10% SOC	90% SOC

Battery	c_1	c_2	c_3	c_4	c_5	c_6
MaxAmps	615.45	791.79	819.87	836.18	955.19	1006.53
Zippy	585.81	735.03	859.25	811.60	983.17	1025.00

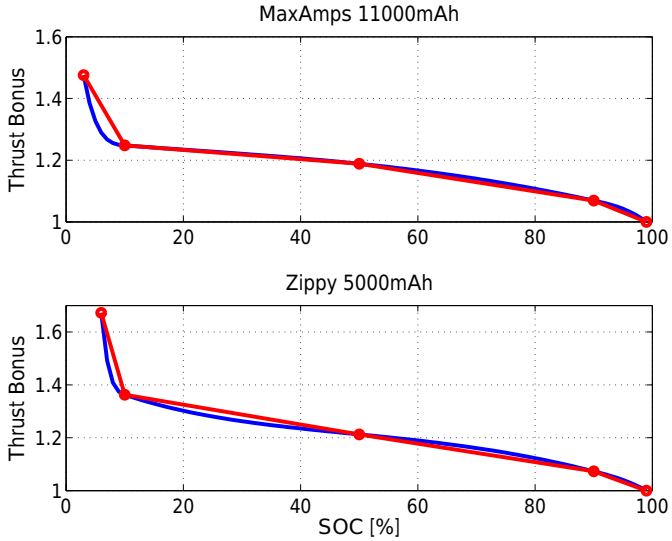

Fig. 14. Inverted nominal thrust and its piecewise-linear approximation

10% SOC). The measured thrust was interpolated using least-squares spline approximation with coefficients from Table I, the two knots were chosen to separate the almost linear piece and two highly non-linear parts.

Assuming that the change in thrust over the SOC is identical for whole range of throttle, it can be normalized. The normalized spline approximation is shown in Figure 13. To obtain function $k_b(SOC)$ ("Thrust-Bonus") of the battery compensator, the normalized throttle curve must be inverted.

To avoid computing a non-linear curve, the inverted thrust bonus is approximated with a piecewise linear function ($y = ax + k$), divided into four segments. The original and linearised curve is shown in Figure 14, the parameters of piecewise linear function, including RMS error of the approximation, are in Table II.

Having these data it is possible to implement the proposed controller.

V. EXPERIMENTAL DATA

The proposed controller was implemented on Arduino board in order to verify the controller performance on the testbench. The controller performance was measured from full battery to 10% SOC to avoid the voltage drop. Both produced thrust and battery output power were measured. The measured thrust was smoothed with EMA

TABLE II. PIECEWISE LINEAR APPROXIMATION OF THE THRUST BONUS

MaxAmps 11000mAh

Segment	Min.SOC	Max.SOC	α	K
1	0	10	-0.0326	1.5737
2	11	50	-0.0015	1.2630
3	51	90	-0.0030	1.3367
4	91	100	-0.0069	1.6900

Zippy 5000mAh

Segment	Min.SOC	Max.SOC	α	K
1	0	10	-0.0775	2.1380
2	11	50	-0.0037	1.4005
3	51	90	-0.0035	1.3880
4	91	100	-0.0073	1.7300

Battery	RMS Error
MaxAmps 11000mAh	33.249
Zippy 5000mAh	32.222

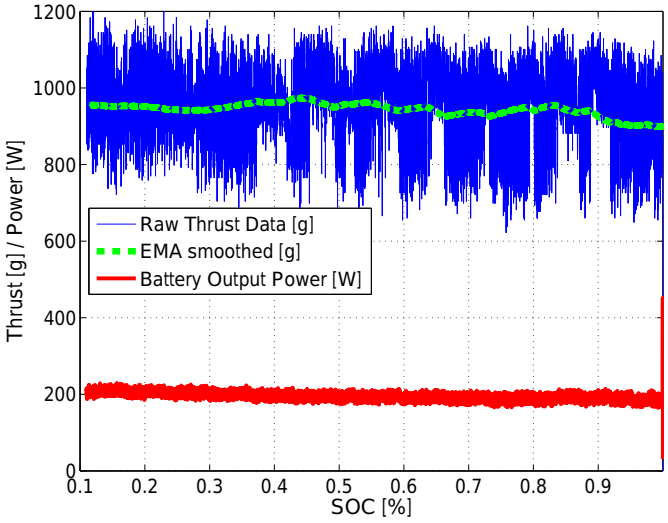

Fig. 15. Laboratory test of the controller with Zippy 5000mAh battery

filter ($\alpha = 0.001$).

The results for Zippy 5000mAh battery is shown in Figure 15, for MaxAmps 11000mAh battery in Figure 16. The overall error of the controller is shown in Table III. *Thrust error* is calculated as the deviation of measured and EMA smoothed thrust from the set value, *Power error* shows the difference of battery output power from its initial value.

The controller performed well in both cases (error under 6%), however MaxAmps battery controller provided dramatically better results (error under 3%). This is because the thrust gain curve for this battery (see that Figure 14 is more linear

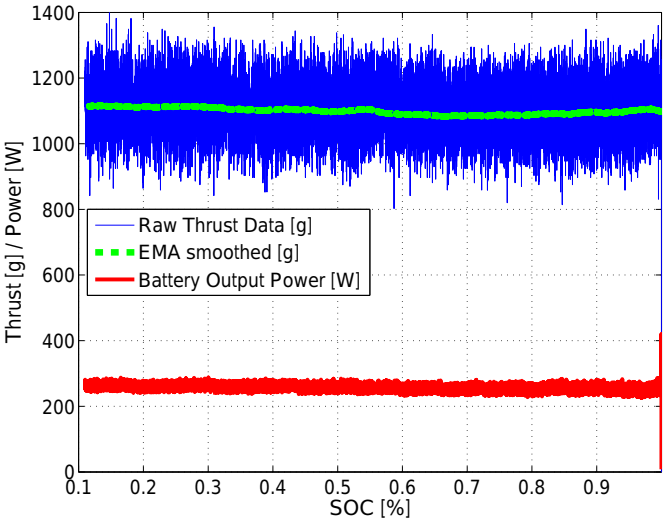

Fig. 16. Laboratory test of the controller with MaxAmps 11000mAh battery

TABLE III. LABORATORY EXPERIMENT ERROR

Battery	Nominal Thrust[g]	Power Error[%]	Thrust Error[%]
Zippy	900	6	10
MaxAmps	1100	3	3

and follows more closely the piecewise linear approximation i.e. the battery dynamics are more linear between 100% and 10% SOC).

VI. CONCLUSION

In this paper a battery model-based thrust controller for small multirotor UAVs was developed and experimentally verified. It takes into account time-varying dynamics of the LiPo batteries and provides control in situation when feedback about actual actuator thrust is not available (such as in multirotor applications).

After characterizing battery dynamics (dependency of nominal thrust on State-of-Charge of the battery), a complete derivation of the controller was shown. To prove the quality of proposed control, a laboratory experiment was conducted. Control errors below 6% for both cases and below 3% for MaxAmps battery were achieved. The linearity of the battery dynamics affects the control performance, showing that better batteries are more linear.

In the future work, this control approach is

to be implemented on a real VTOL platform and verified in actual flight conditions. Although AggieAir platform was used as an example, this controller can be implemented for any VTOL vehicle which uses LiPo batteries.

ACKNOWLEDGMENT

The authors would like to acknowledge Dr. YangQuan Chen of the University of California, Merced; Dr. Rees Fullmer of Utah State University; and Dr. Mac McKee of the Utah Water Research Laboratory.

This work is supported by Utah Water Research Laboratory MLF 2006-2013.

REFERENCES

[1] I.-S. Kim, "The novel state of charge estimation method for lithium battery using sliding mode observer," *Journal of Power Sources*, vol. 163, no. 1, pp. 584–590, Dec. 2006. [Online]. Available: http://www.sciencedirect.com/science/article/pii/S0378775306018349

[2] C. Coopmans, L. Di, A. Jensen, A. A. Dennis, and Y. Chen, "Improved architecture designs for a low cost personal remote sensing platform: Flight control and safety," in Proc. of the ASME Conference*, 2011*, Sep. 2011, pp. 937–943.

[3] C. Coopmans and Y. Han, "Aggieair: An integrated and effective small multi-uav command, control and data collection architecture," in Proc. of the 5th ASME/IEEE International Conference on Mechatronic and Embedded Systems and Applications (MESA09)*, 2009*, 2009, pp. 1–7.

[4] A. Jensen, Y. Chen, M. McKee, T. Hardy, and S. Barfuss, "AggieAir – a low-cost autonomous multispectral remote sensing platform: New developments and applications," in Proc. of the Geoscience and Remote Sensing Symposium (IGARSS)*, 2009*, vol. 4, Jul. 2009, pp. 995–998.

[5] "Utah Water Research Laboratory (web pages)," `http://uwrl.usu.edu/`.

[6] "Paparazzi, the free autopilot (an opensource project)," `http://paparazzi.enac.fr/`.

[7] C. Coopmans, B. Stark, and C. Coffin, "A payload verification and management framework for small UAV-based personal remote sensing systems," in Proc. of the 5th International Symposium on Resilient Control Systems (ISRCS)*, 2012*, Aug. 2012, pp. 184 –189.

[8] J. Barton, "Fundamentals of small unmanned aircraft flight," *Johns Hopkins APL Technical Digest*, vol. 31, no. 2, 2012. [Online]. Available: http://www.jhuapl.edu/techdigest/TD/td3102/31_02-Barton.pdf

[9] S. Bouabdallah and R. Siegwart, "Full control of a quadrotor," in *IEEE/RSJ International Conference on Intelligent Robots and Systems, 2007. IROS 2007*. IEEE, Nov. 2007, pp. 153–158.

[10] "Universal state-of-charge indication for battery-powered applications," in *Battery Management Systems*, ser. Philips Research Book Series. Springer Netherlands, 2008, p. 3.

[11] B. Bhangu, P. Bentley, D. Stone, and C. Bingham, "Observer techniques for estimating the state-of-charge and state-of-health of VRLABs for hybrid electric vehicles," in Proc. of the Vehicle Power and Propulsion*, 2005*, Sep. 2005, pp. 10–15.

[12] S. Pang, J. Farrell, J. Du, and M. Barth, "Battery state-of-charge estimation," in Proc. of the American Control Conference*, 2001*, vol. 2, 2001, pp. 1644 –1649.

[13] K. Hatzel, "A survey of long-term health modeling, estimation, and control of lithium-ion batteries: Challenges and opportunities," in Proc. of the American Control Conference (ACC)*, 2012*, 2012, pp. 584–591.

[14] S. Weiss, D. Scaramuzza, and R. Siegwart, "Monocularslambased navigation for autonomous micro helicopters in gpsdenied environments," *Journal of Field Robotics*, vol. 28, no. 6, pp. 854–874, 2011. [Online]. Available: http://www.jhuapl.edu/techdigest/TD/td3102/31_02-Barton.pdf

[15] J. Stowers, M. Hayes, and A. Bainbridge-Smith, "Altitude control of a quadrotor helicopter using depth map from microsoft kinect sensor," in *2011 IEEE International Conference on Mechatronics (ICM)*, Apr. 2011, pp. 358 –362.

[16] D. Eynard, P. Vasseur, C. Demonceaux, and V. Fremont, "UAV altitude estimation by mixed stereoscopic vision," in *2010 IEEE/RSJ International Conference on Intelligent Robots and Systems (IROS)*, Oct. 2010, pp. 646 –651.

[17] A. Cherian, J. Andersh, V. Morellas, N. Papanikolopoulos, and B. Mettler, "Autonomous altitude estimation of a UAV using a single onboard camera," in *IEEE/RSJ International Conference on Intelligent Robots and Systems, 2009. IROS 2009*, Oct. 2009, pp. 3900 –3905.

[18] P. Pounds, R. Mahony, and P. Corke, "System identification and control of an aerobot drive system," in *Information, Decision and Control, 2007. IDC '07*, Feb. 2007, pp. 154 –159.

[19] C. Cheron, A. Dennis, V. Semerjyan, and Y. Chen, "A multifunctional HIL testbed for multirotor VTOL UAV actuator," in Proc. of the IEEE/ASME International Conference on Mechatronics and Embedded Systems and Applications (MESA)*, 2012*, Jul. 2010, pp. 44 –48.

[20] K. Alexis, G. Nikolakopoulos, and A. Tzes, "Model predictive quadrotor control: attitude, altitude and position experimental studies," *IET Control Theory Applications*, vol. 6, no. 12, pp. 1812 –1827, 2012.

[21] H. Bouadi, S. Simoes Cunha, A. Drouin, and F. Mora-Camino, "Adaptive sliding mode control for quadrotor attitude stabilization and altitude tracking," in *2011 IEEE 12th International Symposium on Computational Intelligence and Informatics (CINTI)*, Nov. 2011, pp. 449 –455.

[22] B.-C. Min, J.-H. Hong, and E. Matson, "Adaptive robust control (ARC) for an altitude control of a quadrotor type UAV carrying an unknown payloads," in *2011 11th International Conference on Control, Automation and Systems (ICCAS)*, Oct. 2011, pp. 1147 –1151.

[23] Y. Hu and S. Yurkovich, "Battery state of charge estimation in automotive applications using LPV techniques," in Proc. of the American Control Conference (ACC)*, 2010*, Jul. 2010, pp. 5043 –5049.